Two-Mode Rhomboidal States in Driven Surface Waves

H. Arbell and J. Fineberg

The Racah Institute of Physics, The Hebrew University of Jerusalem, Jerusalem 91904, Israel

(Received 19 May 1999)

Two-mode rhomboid patterns are generated experimentally via two-frequency parametric forcing of surface waves. These patterns are formed by the simple nonlinear resonance: $\vec{k}_2' - \vec{k}_2 = \vec{k}_1$ where k_1 and $k_2 (= k_2')$ are concurrently excited eigenmodes. The state possesses a direction-dependent time dependence described by a superposition of the two modes, and a dimensionless scaling delineating the state's region of existence is presented. We also show that $2n$-fold quasipatterns naturally arise from these states when the coupling angle between $\vec{k}_2$ and $\vec{k}_2'$ is $2\pi/n$.

PACS numbers: 47.54.+r, 47.20.Gv, 47.35.+i, 47.52.+j

Pattern-forming systems often result from nonlinearly interacting waves. The simplest nonlinear pattern-forming systems are those in which a single wave number becomes unstable. Our understanding of these "single-mode" systems is now well developed. In many situations, however, numerous *different* modes may be concurrently excited. The simplest example of a "multimode" nonlinear system is, of course, when two distinct wave numbers are simultaneously excited. This important class of systems has only recently begun to be investigated. The space of nonlinear states that can result is quite rich, as recent experimental observations of both quasicrystalline patterns [1] and nonlinear superlattice states [2,3] suggest.

Are these the only types of patterns that a two-mode system can form, and can one characterize the nonlinear mechanisms that form them? Here we report the first experimental observation of the spontaneous formation of a nonlinear state exhibiting rhomboidal patterns, formed as a result of resonant three-wave coupling between wave vectors with distinctly different wave numbers. Although predicted to occur in a variety of nonlinear systems, this state has only previously been observed in a nonlinear optical system where the orientations of the interacting wave vectors [4] were externally imposed. Below we show that rhomboidal patterns coupling two wave vectors of length k_2 with one wave vector of length k_1 evolve *spontaneously* from two circles of linearly degenerate states. These states have both interesting temporal dynamics and provide a mechanism for the appearance of two-frequency quasicrystalline patterns, which naturally evolve from rhomboidal patterns when an additional resonance condition is met.

Two qualitatively different types of rhombic systems have been predicted to exist in driven nonlinear systems. The first of these results from slight distortions of a hexagonal state. These "distorted hexagons" are predicted to be stable in models that possess quadratic terms with a derivative coupling [5,6]. Despite the global stability of hexagonal states, distorted hexagons were shown in [6] to be locally stable due to a local energy barrier preventing their transition to hexagons. They may arise due to either initial or boundary conditions [7]. Possible experimental realizations of this mechanism are rhombic states observed in reaction-diffusion systems [6], convection in an imposed shear flow [8], and flux line lattices in superconductors [9].

A second type of nonlinear rhombic patterns results from the nonlinear interaction of waves with significantly different wavelengths. Such states have been observed numerically in a Swift-Hohenberg model possessing two unstable wave numbers [10]. They have also been theoretically anticipated in anisotropic models where two unstable degenerate wave vectors are resonant with an externally imposed wave number [11], in nonlinear optical systems [12,13], and in the analysis of the Faraday instability excited with two frequencies [14].

In our experiments we use the Faraday instability to study two-mode nonlinear wave interactions. Beyond a critical vertical (parallel to $\vec{g}$) acceleration, vibration of a fluid layer of depth, h, with angular frequency ω excites a pattern of wave number k on the fluid surface. To study the interactions of two distinct wave numbers, k_1 and k_2, we excite the system with two commensurate frequencies, $\omega_1 = m\omega_0$ and $\omega_2 = n\omega_0$, where $n > m$ are mutually prime integers. The excitation acceleration has the form:

$$A[\cos(\chi)\cos(m\omega_0 t) + \sin(\chi)\cos(n\omega_0 t + \phi)], \quad (1)$$

where the angle χ, describes the degree of mixing between the two modes.

Our working fluids were Dow-Corning 200 silicone oils with kinematic viscosities ν of 8.7, 23, 47, 87 cS and TKO-77 vacuum pump fluid with $\nu = 184$ cS at respective temperatures of 30 and 33 $\pm$ 0.05 °C. The apparatus and imaging system are described in detail in [2]. We performed our experiments in circular fluid layers of diameter 14.4 cm with $0.1 < h < 0.55$ cm where pattern correlation lengths [1] are typically much less than the system size. Our imaging system provides visualization of the absolute value of the local slope along the fluid surface. A 1 msec shutter enabled instantaneous visualization of the fluid states. We also performed high resolution measurements of the surface slope at a single point by measuring the location of a reflected laser beam with a position sensitive detector [15]. This method yields an accuracy of 1%–5% in the surface slope at the point of reflection.

 0031-9007/00/84(4)/654(4)$15.00

Below we describe two wave-number rhombic ($2kR$) states generated with $n{:}m = 3{:}2$ and $12 < \omega_0/2\pi < 45$ Hz. In experiments with frequency combinations (in Hz) 50/25, 60/30, 80/40, 56/40, 63/45, 68/48, 70/50, 75/55, 77/55, 50/30, 70/40, 60/45, 65/50, 80/50, 68/52, 84/60, and 100/60, $2kR$ states were *not* observed.

In Fig. 1 we present a typical image of a $2kR$ pattern. Although k_1 and k_2 are the linearly unstable wave numbers [16] excited by the $3\omega_0$ and $2\omega_0$ driving frequencies, their specific orientation, hence the type of pattern selected by the system, is determined by their nonlinear interactions. This nonlinear state is formed by the resonant triad, $\vec{k}_2' - \vec{k}_2 = \vec{k}_1$, where $|\vec{k}_2'| = |\vec{k}_2| = k_2$ and $|\vec{k}_1| = k_1$. The higher harmonics seen are an artifact of the imaging and can be reproduced by computer simulation. A similar three-wave resonance occurs for 2:1 forcing; instead of the $\vec{k}_2' - \vec{k}_2 = \vec{k}_1$ (vector difference) resonance, an additive $\vec{k}_1' + \vec{k}_1 = \vec{k}_2$ resonance governs the selected pattern. The resulting pattern (not shown) is a superposition of hexagonal lattices composed of the two scales. These two types of three-wave resonances are consistent with predictions by Silber and Skeldon [14] based on symmetry considerations. In [14] three-wave interactions with additive resonant coupling are allowed *only* for (even-odd) frequency ratios, such as 2:1, where the higher frequency is an even multiple of ω_0. For odd-even forcing, such as 3:2, no additive triad interactions can occur. A similar analysis predicts three-wave resonant coupling based on vector differences (such as $\vec{k}_2' - \vec{k}_2 = \vec{k}_1$) can occur only for odd-even forcing.

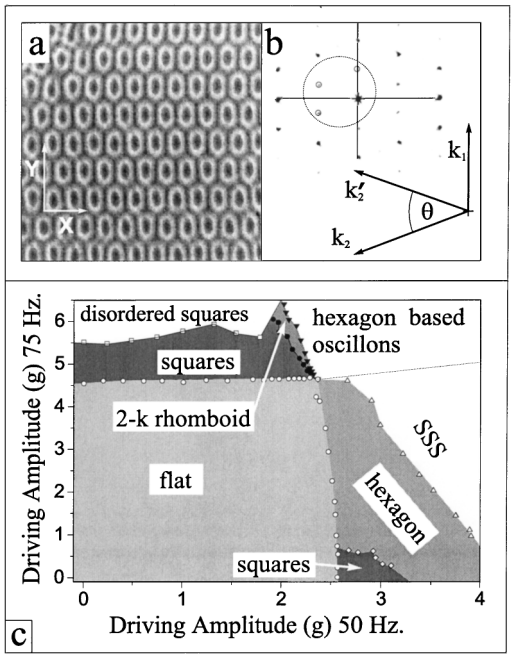

FIG. 1. (a) A typical image of the $2k$ rhomboid ($2kR$) state observed for parameters: $\omega_0/2\pi = 25$ Hz, $\nu = 23$ cS, and $h = 0.2$ cm. The axis y gives the direction of the "compressed" vector. (b) Power spectrum of (a). The circled wave vectors (bottom right) illustrate the simple resonance condition $\vec{k}_2' - \vec{k}_2 = \vec{k}_1$ which creates the grid in k space. The two vectors $\vec{k}_2'$ and $\vec{k}_2$ correspond to the $3\omega_0/2$ component while $\vec{k}_1$ corresponds to $2\omega_0/2$. θ here is 41°. (c) A typical phase diagram ($\omega_0/2\pi = 25$ Hz, $h = 0.2$ cm, $\nu = 23$ cS, $\phi = 0$). Symbols describe the measured transitions. Besides the square, hexagon, and SSS reported previously [2], we observe $2kR$ and an additional new state, hexagonal based oscillons (HBO) [19].

A typical phase space in which $2kR$ rhomboids are observed is presented in Fig. 1(c). As in most studies of two-frequency driving [1,17], two main regions, dominated by either k_1 or k_2, exist. At a critical value of $\chi = \chi_c$, a bicritical point exists where both wave numbers are linearly unstable. In this vicinity, the waves can interact to form a variety of different nonlinear states. Away from χ_c, the phase diagram is similar to [2]. Square patterns exist in the k_2-dominant and strongly k_1-dominant regions. Hexagonal patterns, which bifurcate into subharmonic superlattice states (SSS) [2], appear for $\chi < \chi_c$. (SSS result from the nonlinear coupling of the dominant of the two excited modes with its own subharmonic mode.) In the vicinity of χ_c, however, the $2kR$ state exists in a triangular region of phase space, bounded from below by squares of wave number k_2 and above by a novel state of oscillons (i.e., very high-amplitude localized waves [18]) that appear on an underlying hexagonal wave state with k_1 the dominant wave number. A detailed description of these states will be presented elsewhere [19].

At the lower boundary of the $2kR$ area the pattern is not always correlated over the entire system and $2kR$ (or variants of this structure) can sometimes be found in two or three domains. When two domains are formed, the angle between them is the same as the angle θ separating $\vec{k}_2$ and $\vec{k}_2'$ [see Fig. 1(b)]. This behavior also occurs in "knitting patterns" [20], formed near a bistable point of triblock copolymer configurations. (These new materials have a reciprocal lattice structure similar to $2kR$ states.) As A is increased, the $2kR$ domains merge into a single domain. Further increase of A yields a hysteretic bifurcation to the "hexagon based oscillon" state (HBO). As the two driving frequencies are commensurate, the phase variable ϕ in Eq. (1) is a relevant control parameter. Typically, the $2kR$ state exists over the range $-20° < \phi < +15°$. The phase space presented in Fig. 1(c) is typical for $0.16 < h < 0.22$ cm, $\omega_0/2\pi > 20$ Hz, and $\nu = 23$ cS.

At higher values of ν and h a slightly different scenario exists. As in Fig. 1(c) square and hexagonal patterns still exist close to onset for, respectively, $\chi > \chi_c$ and $\chi < \chi_c$. Upon the increase of A, however, both types of patterns become rolls. The appearance of the $2kR$ state is, however, unaffected by the state preceding it. They still appear for a similar range of ϕ. The HBO also remain. In general, the size of the region in phase space where a single $2kR$ domain exists decreases with the distance from $\phi = 0$.

For values of ϕ outside of the range of existence of $2kR$, either 2MS or unlocked states appear. 2MS states [2] are characterized by the spatial resonance $\vec{k}_2 - \vec{k}_1 = \vec{k}_3$,

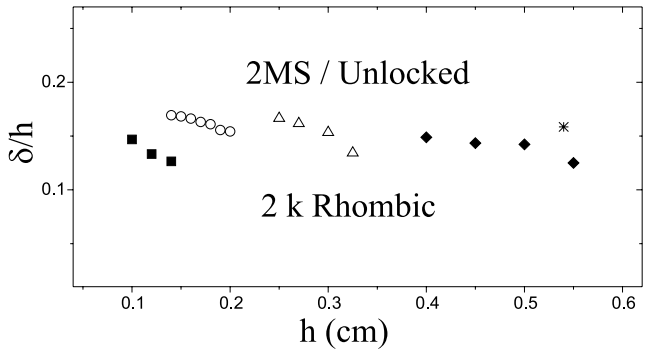

FIG. 2. The transition points between the regions of $2kR$ and 2MS/unlocked for $\phi = 0$. We plot the dimensionless parameter δ/h [21] as a function of the fluid layer height, h, for (squares) $\nu = 8.7$, (circles) $\nu = 23$, (triangles) $\nu = 47$, (diamonds) $\nu = 87$, and (asterisk) $\nu = 184$ cS.

where k_3 is a linearly *stable* wave number whose magnitude is determined by the dispersion relation, $k_3 = k(\omega_3/2)$ and temporal resonance $\omega_3 = \omega_2 - \omega_1$. In the "unlocked" type states [2] k_1 and k_2 both exist concurrently, but no defined temporal or spatial phase relation between them exists. The nontrivial ϕ dependence of the pattern observed here has also been seen in [1,3,17].

To gain a better understanding of the domain of existence of the $2kR$ we measured the ω_0, ν, and h dependence of the transition from the rhomboid state to the 2MS/unlocked states for $\phi = 0$. The results can be seen in Fig. 2 where we plot the dimensionless quantity, δ/h at the transition from rhomboids to 2MS states as a function of both h and ν. $\delta \equiv (\nu/\omega_{ave})^{1/2}$ where $\omega_{ave} \equiv (\omega_2 - \omega_1)/2$. As the figure shows, a transition occurs at $\delta/h \sim 0.15$. Above (below) this value 2MS/unlocked ($2kR$) states exist. The parameter δ/h was also shown to be important for pattern selection by single frequency excitations [21].

By varying ν, h, and ω_0 it is possible to tune both the ratio k_2/k_1 and the angle θ (see Fig. 1) of the $2kR$ state. In our experiments we obtained values of $\theta = 41°$ ($h = 0.20$ cm, $\nu = 23$ cS), $36°$ ($h = 0.33$ cm, $\nu = 47$ cS), $32°$ ($h = 0.53$ cm, $\nu = 100$ cS), and $29°$ ($h = 0.53$ cm, $\nu = 183$ cS). The Faraday instability is known to produce quasicrystalline patterns in some regions of phase space, where 8-, 10-, and 12-fold patterns have been observed [1,22]. As suggested by [23], a quasicrystalline state can be naturally generated when $360/\theta = n$, as then an integer number of triads could be formed. As conjugate pairs of triads are always formed, the integer n must always be even (as observed in [1,10]) in this scenario. As Fig. 3 (left) shows, the formation of perfect tenfold quasicrystalline patterns indeed occurs when this condition is satisfied. As the power spectrum in Fig. 3 (center) indicates, each of the inner circle of peaks of magnitude k_1 is coupled by a triad resonance with two peaks of magnitude k_2 along the outer circle. It is interesting to note that when $\theta \approx 41°$, where a symmetric quasipattern is not possible, we observe a distorted eightfold quasipattern such as the one in Fig. 3 (right).

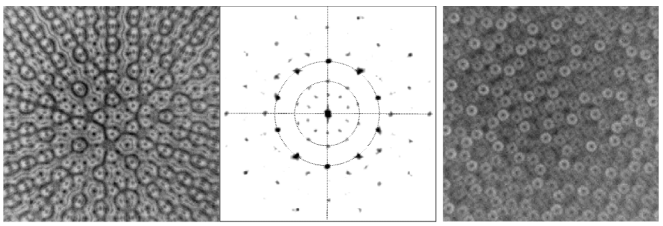

FIG. 3. (left) A tenfold quasiperiodic pattern and its power spectrum (center) is observed for $\omega_0/2\pi = 30$ Hz, $\nu = 47$ cS, and $h = 0.33$ cm. Circles are drawn with radii k_1 (inner) and k_2 (outer). For these parameters $\theta = 360°/10$ and five $2kR$ regions combine to form the quasipattern. For $\omega_0/2\pi = 30$ Hz, $\nu = 23$ cS, and $h = 0.2$ cm (right) an *apparent* eightfold symmetric pattern is seen. However this pattern is actually a deformed quasipattern since the $2kR$ value here of $\theta = 41°$ does not evenly divide 360°.

The temporal behavior of the $2kR$ state is interesting. Figure 4 shows a typical time series of the x and y components of the surface gradient of this state at a single point. (The $x||\vec{k}_1$ and y directions are defined in Fig. 1.) In contrast to the simple periodic behavior of the standing wave patterns generated by single frequency excitation, each direction of the $2kR$ state exhibits *different* time dependence. In a given direction, the time dependence corresponds to the temporal behavior of eigenvectors with components in that direction. The overall time dependence of the surface height h can be described by

$$\begin{aligned} h(t,x,y) =& [a_1\cos(\omega_0 t) + a_2\cos(2\omega_0 t) + \cdots]\cos(\vec{k}_1\cdot\vec{x}) \\ &+ [b_1\cos(\omega_0 t/2) + b_2\cos(3\omega_0 t/2) + \cdots] \\ &\times [\cos(\vec{k}_2\cdot\vec{y}) + \cos(\vec{k}_2'\cdot\vec{y})]. \end{aligned} \tag{2}$$

An arbitrary x, y point will contain the time behavior of both the k_1 or k_2 eigenfunctions. By our choice of axes, the $\partial_x h$ component contains mainly the $\omega_1/2$,

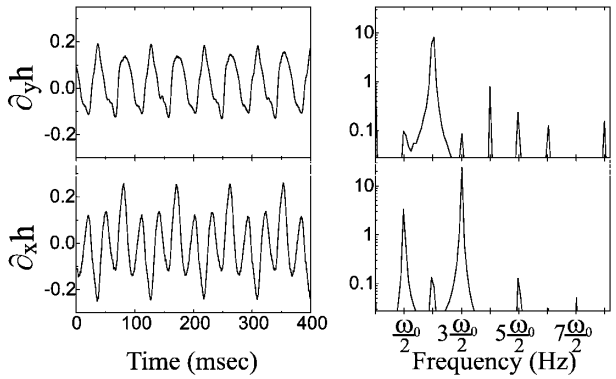

FIG. 4. The time dependence of the $2kR$ state was studied using the reflection of a laser by the surface waves. The directional derivatives $\partial_x h, \partial_y h$ as a function of time (left) and their corresponding power spectra (right) show that each direction has a different temporal dependence. [The x, y directions are defined in Fig. 1(a).] $\partial_y h$ is dominated by the k_2 and k_2' components and $\partial_x h$ corresponds to the k_1 component. The parameters for the above were $\omega_0/2\pi = 22$ Hz, $\nu = 23$ cS, $\phi = 0$, and $h = 0.2$ cm.

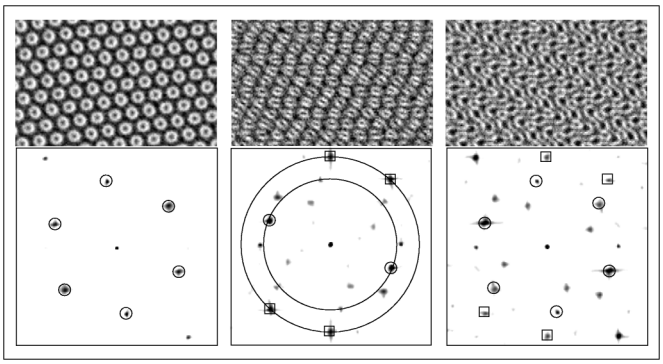

FIG. 5. A typical sequence of images (upper) and their power spectrum (lower) taken for the $2kR$-hexagon state that appears for $\nu = 8.7$ and $0.1 < h < 0.2$ cm. For fixed parameters each temporal phase appears different as the state changes from (right) a pure, k_1 dominant, hexagonal phase to (center) a $2kR$ phase and (right) a combination of both. Similar states were also observed in 4:5 forcing.

$2\omega_1/2, \ldots$ (note: $\omega_1 = 2\omega_0$, $\omega_2 = 3\omega_0$) peaks, while the dominant frequencies in the y direction are $(\omega_2 - \omega_1)/2$, $\omega_2/2, \ldots$. When a *single* mode is dominant, the predictions of [24] are in good quantitative agreement with our measurements of the relative peak intensities. In the regime where two modes are concurrently excited, [24] is inapplicable, and a new theoretical framework is needed.

For $\nu = 8.7$ cS, $0.1 < h < 0.2$ cm, and $\delta/h < 0.13$, in place of the pure $2kR$ state an interesting variant is observed whose symmetry changes with its temporal phase. This is shown in Fig. 5 where a time sequence is presented for fixed experimental parameters. For different temporal phases pure hexagonal (left), rhomboid dominant (center), and mixed hexagonal and $2kR$ (right) are seen. Together with the vector triad characteristic of $2kR$, coupling with the difference vector, $\vec{k}_2 - \vec{k}_1$, is also observed in the spatial spectrum. This state exists for a significantly broader range of ϕ ($-70 < \phi < 70$) than the pure rhomboidal state.

As demonstrated above, the space of nonlinear patterns formed by two interacting unstable modes is very rich. Our understanding of the types of structures and their selection is just beginning. Predicted nonlinear three-wave resonances [14], however, appear to govern nonlinear pattern selection only for the *simplest* ratios (3:2 and 2:1). Although a quantitatively accurate [24] theory exists in regimes where a single mode is dominant, a quantitative theory for the important regime of two or more concurrently unstable modes is lacking.

We acknowledge the support of the Israel Academy of Sciences (Grant No. 203/99).

[1] W. S. Edwards and S. Fauve, Phys. Rev. E **47**, 788 (1993).
[2] H. Arbell and J. Fineberg, Phys. Rev. Lett. **81**, 4384 (1998).
[3] A. Kudrolli and J. P. Gollub, Physica (Amsterdam) **123D**, 99 (1998).
[4] A. V. Mamaev and M. Saffman, Phys. Rev. Lett. **80**, 3499 (1998).
[5] E. A. Kuznetsov, A. A. Nepomnyashchy, and L. M. Pismen, Phys. Lett. A **205**, 261 (1995).
[6] G. H. Gunaratne, Q. Ouyang, and H. L. Swinney, Phys. Rev. E **50**, 2802 (1994).
[7] P. C. Matthews, Physica (Amsterdam) **116D**, 81 (1998).
[8] P. Hall and R. E. Kelly, Phys. Rev. E **52**, 3687 (1995).
[9] M. Yethiraj, D. M. Paul, C. V. Tomy, and E. M. Forgan, Phys. Rev. Lett. **78**, 4849 (1997).
[10] R. Lifshitz and D. M. Petrich, Phys. Rev. Lett. **79**, 1261 (1997).
[11] R. Schmitz and W. Zimmermann, J. Phys. (Paris) II **7**, 677 (1997).
[12] A. J. Scroggie and W. J. Firth, Phys. Rev. A **53**, 2752 (1996).
[13] M. Hoyuelos, P. Colet, M. San Miguel, and D. Walgraef, Phys. Rev. E **58**, 2992 (1998).
[14] M. Silber and A. C. Skeldon, Phys. Rev. E **59**, 5446 (1999).
[15] We measure the surface slope with a modulated (at 50 KHz) 30 mW diode laser. A 50 mm Canon f/1.2 lens imaged the reflected beam onto a UDT SL20 PSD sensor, whose output, digitized to 12 bit resolution at 10 kHz, yielded the beam's location. The fluid surface gradient at a specific point was then calculated.
[16] K. Kumar and L. S. Tuckerman, J. Fluid Mech. **279**, 49 (1994); T. Besson, W. S. Edwards, and L. S. Tuckerman, Phys. Rev. E **54**, 507 (1996).
[17] H. W. Muller, Phys. Rev. Lett. **71**, 3287 (1993).
[18] P. Umbanhowar, F. Melo, and H. L. Swinney, Nature (London) **382**, 793 (1996); O. Lioubashevski, Y. Hamiel, A. Agnon, Z. Reches, and J. Fineberg, Phys. Rev. Lett. **83**, 3190 (1999).
[19] H. Arbell and J. Fineberg (to be published).
[20] U. Breiner, U. Krappe, E. L. Thomas, and R. Stadler, Macromolecules **31**, 135 (1998).
[21] O. Lioubashevski, H. Arbell, and J. Fineberg, Phys. Rev. Lett. **76**, 3959 (1996); O. Lioubashevski, J. Fineberg, and L. S. Tuckerman, Phys. Rev. E **55**, 3832 (1997).
[22] B. Christiansen, P. Alstrom, and M. T. Levinsen, Phys. Rev. Lett. **68**, 2157 (1992); D. Binks and W. van de Water, Phys. Rev. Lett **78**, 4043 (1997).
[23] T. Frisch and G. Sonnino, Phys. Rev. E **51**, 1169 (1995).
[24] W. Zhang and J. Vinals, J. Fluid Mech. **341**, 225 (1997).